

# Global Structure of the El Niño/Southern Oscillation

## Part I. El Niño Composites

By Tetsuzo Yasunari\*

*Department of Meteorology, Florida State University, Tallahassee, FL32306  
(Manuscript received 19 August 1986, in revised form 19 December 1986)*

### Abstract

The three dimensional structures of sea surface temperature (SST) and atmospheric circulation anomalies associated with ENSO are investigated over the entire globe, by using the objectively analyzed data sets of the years 1964 to 1981. The global data sets of U, V, Z and T are produced by applying the least-square method to fit the time-filtered station data (of more than 320 stations) and NMC tropical wind field data with truncated spherical harmonics of wavenumber 0 to 5. Global SST and sea level pressure data are also utilized. In this paper (Part I) the composite anomaly patterns during El Niño episodes are discussed.

Warm SST anomalies and warm upper troposphere are found to be remarkable not only over the equatorial central Pacific but also over the entire tropics, while the mid-latitudes seem to be characterized as cold SST and cold troposphere as a whole. The increasings of zonal winds in the subtropics and the lower mid-latitudes of the two hemispheres are also prominent. These evidences apparently suggest that the intensified Hadley-type circulation in the low latitudes and the equatorward extent of the circumpolar vortex in the high latitudes are fundamental features during El Niño episodes. A nearly symmetric response pattern of the upper tropospheric flows with respect to the equator is also noted over the northern and the southern Pacific.

It is also suggested that the North Atlantic Oscillation (NAO) is synchronized with the SO during the present analysis period.

### 1. Introduction

In recent years, the El Niño/Southern Oscillation (ENSO) has become of great interest as a typical prototype of large-scale atmosphere-ocean interaction. This phenomenon was described first by Walker and Bliss (1932) and was physically conceptualized first by Bjerknes (1966). The 1982/83 El Niño, which was one of the largest events in this century has induced renewed interest in this phenomenon.

Another remarkable aspect of ENSO may be the distinct climatic anomalies over the north Pacific through north America (Bjerknes, 1969; Namias, 1976; Horel and Wallace, 1981 etc.), associated with the extreme phases (*i.e.*, El Niño or anti-El Niño) over the equatorial eastern

Pacific. These anomalies have now been understood as stationary Rossby wave responses to the anomalous heat source over the equatorial Pacific (*e.g.*, Blackmon *et al.*, 1983; Shukla and Wallace, 1984 etc.). A theoretical background of this problem was given by Hoskins and Karoly (1981).

The current unresolved problem on ENSO is what is the physical mechanism of the ENSO cycle with a period of several years. A number of coupled ocean-atmosphere models have now been proposed to simulate the tropical aspects of ENSO, particularly the time evolution of SST and wind field along the tropical Pacific region.

Philander *et al.* (1984) simulated eastward propagation of sea surface temperature (SST) and wind field with linear dynamics for both the ocean and atmosphere. Their results seem to agree fairly well with the observations over the

\*Present Affiliation: Institute of Geoscience, University of Tsukuba, Ibaraki 305, Japan.

equatorial Pacific during 1982/83, though this model does not describe the ENSO cycle.

Anderson and McCreary (1985) proposed a model with non-linear ocean dynamics and linear atmosphere dynamics. They first showed the cycle, namely from El Niño to anti-El Niño and from anti-El Niño to El Niño in the SST and wind fields, though some features are quite different from the observations.

Zebiak and Cane (1985) proposed a more sophisticated model including the seasonal cycle and prediction equation of SST. This model seems to have successfully simulated the SST and wind field evolutions in the ENSO cycle with some periodicity (but with the time scale of several years), though the zonal propagation of their wind field seems to be opposite to the observed field (Gill and Rasmusson, 1983). They stressed that the ENSO can fundamentally be described as the atmosphere-ocean interaction over the tropical Pacific.

However, some recent observational studies have presented distinct evidences of the ENSO related anomalies outside the tropical Pacific region, which precede the extreme phases over the equatorial eastern Pacific (*i.e.*, El Niño or anti-El Niño events) with one or two seasons or more. Barnett (1983, 1984a, 1984b, 1985) offered evidences of eastward propagations of surface wind and pressure anomalies from the equatorial Indian Ocean toward the central Pacific. Krishnamurti *et al.* (1986) showed the global link of the surface pressure anomalies related to the ENSO cycle. Their results on the tropical belt seem to be similar to those of Barnett (1985).

Yasunari (1985) presented the evidences of eastward propagations of the tropical east-west anomalous circulation associated with ENSO. The propagation of the anomalies of zonal and divergent wind fields seem to be consistent with the surface fields by Barnett and Krishnamurti *et al.* Very recently, Gutzler and Harrison (1986) showed a very similar feature to Yasunari's by using different statistical approach. van Loon and Shea (1985) noted the significant ENSO related signals in the sea-level pressure, temperature and wind over the eastern Indian Ocean through Australia south of 15°S, preceding the typical El Niño (or anti-El Niño). These studies strongly

suggest that the preceding signals to ENSO do exist outside the tropical Pacific region.

In addition, a strong association of Indian summer monsoon with ENSO (Pant and Parthasarathy, 1981; Rasmusson and Carpenter, 1983; Bhalme and Jadhav, 1984 etc.) suggests us some physical link (not a one-way response) between the tropics and extra-tropics with this time scale. To understand the total physical process of the ENSO, therefore, the time evolution of atmospheric (and oceanic) parameters in the whole ENSO cycle should be examined for the entire globe.

The present study will focus on this problem based on the analysis of the objectively analyzed atmospheric circulation parameters and SST associated with the ENSO over the global grids. This paper (Part I) will describe the objective analysis scheme and will assess the anomalies during El Niño (or anti-El Niño). Part II will describe the time evolution of SST and atmosphere during the course of ENSO cycle and will discuss a possible physical process of the ENSO.

## 2. Data sets

Main data source for wind, temperature and geopotential height is based on Monthly Climatic Data for the World (Upper Air Data) covering the period from January 1964 to December 1981. We selected 320–340 stations which contain more than two thirds of the total records. National Meteorological Center (NMC)'s tropical operational wind field analysis (48.1°N–48.1°S) are adopted for the period of 1968 to 1981 to cover data sparse oceanic regions. This data incorporates satellite-derived cloud winds as well as winds observed by commercial aircrafts.

Monthly mean 10° × 10° gridded global sea level pressure (SLP) data set compiled by Krishnamurti *et al.* (1986) are also utilized. Monthly mean global SST data compiled at NOAA (Reynolds, 1983) are also used.

## 3. Objective analysis of time filtered data

During the analysis period (1964–1981), El Niño/Southern Oscillation (ENSO) cycle prominently shows the periodicity of 3 to 5 years, as demonstrated in the Southern Oscillation Index (SOI) (Fig. 1) defined as the SLP difference of

Tahiti minus Darwin. To extract the anomalies purely related to ENSO cycles, a recursive time filter (M. Murakami, 1981) with the frequency response of 30–60 month period with the maximum response of 45 month period (Fig. 2) was applied to all the data sets described in section 2. Mean seasonal cycles were subtracted from the original monthly data before we applied the time filter.

Time filtered U and V components of winds at 700 mb and 200 mb for 320 stations and 80 grids of NMC wind data are then objectively analyzed by using the least-square method following Pan (1979).

For each month of the analysis period,  $K$  points observations, *e.g.*  $[u_k]: k=1, 2, \dots, K$  are given. In this case, the observation number  $K$  are 400. The location for the  $K$ -th point is given by  $\lambda$  the longitude and  $\theta$ , the co-latitude. The objective analysis field are defined as the function

$$u(\lambda, \theta) = \sum_{m=0}^M \sum_{n=m}^{m+N} [A_{mn} \cos(m\lambda) + B_{mn} \sin(m\lambda)] P_n^m(\cos \theta) \quad (1)$$

where  $P_n^m(\cos \theta)$  represents the associated Legendre function. The coefficients  $A_{mn}$  and  $B_{mn}$  are obtained by fitting the data set  $[u_k]$  in such a way as to make

$$S = \sum_{k=1}^K \alpha_k^2 (u_k - u(\lambda_k, \theta_k))^2 \quad (2)$$

a minimum with respect to each of the coefficients  $A_{mn}$  and  $B_{mn}$ , that is

$$\frac{\partial S}{\partial A_{mn}} \equiv 0 \quad (3)$$

where  $0 \leq m < M, m \leq n \leq m + M$  and

$$\frac{\partial S}{\partial B_{mn}} \equiv 0 \quad (4)$$

where  $1 \leq m < M, m \leq n \leq m + M$

The details to solve the equations (3) and (4) are described minutely in Pan (1979). The  $\alpha$  are Gauss' precision moduli. The function  $u(\lambda, \theta)$  represents a truncated series of surface spherical harmonics. The index  $m$  represents the zonal wavenumber while  $n-m$  represents the meridional wavenumber, or the number of zero points between the two poles.

In spectral numerical models, two types of truncation have been used; *i.e.*, the rhomboidal and the triangular truncations. In this study the rhomboidal truncation is adopted here simply because

- 1) it gives equal number of degree of freedom to each zonal wavenumber
- 2) resolution in higher latitudes are relatively better than the triangular truncation.

There may be at least two factors for determining the truncation limit  $M$  (or the maximum zonal wavenumber). One may be the over-deter-

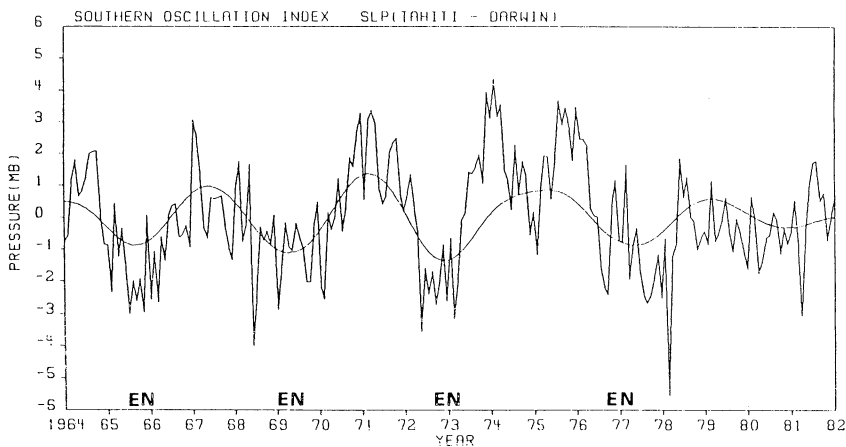


Fig. 1. Southern Oscillation Index (Tahiti minus Darwin sea level pressure) and its time filtered series. El Niño phases are shown with "EN".

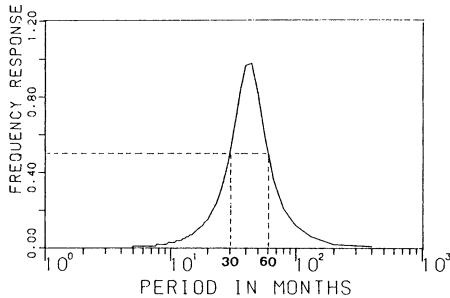


Fig. 2. Frequency response of time filter adopted here. Periods of half response (30 months and 60 months period) are also indicated.

mination factor (*i.e.*, number of data/number of coefficients) for the least-square method. This number should be as large as possible. Another factor may be space-scales of anomalies that should be described in spherical surface. Since the anomalies associated with the Southern Oscillation may be of planetary-scale, the maximum zonal wavenumber  $M$  is chosen to be 5, which totally gives 66 coefficients. The corresponding over-determination factor is about 5, which may be sufficient for the least-square method.

By using A and B thus obtained, Fourier coefficients of zonal waves for each latitude are calculated as follows:

$$C_m(\theta) = \sum_{n=m}^{m+M} A_{m,n} P_n^m(\cos \theta) \quad (5)$$

and

$$D_m(\theta) = \sum_{n=m}^{m+M} B_{m,n} P_n^m(\cos \theta) \quad (6)$$

Finally, the analyzed field of  $u(\lambda, \theta)$  are obtained as follows:

$$\begin{aligned} & \dot{u}(\lambda, \theta) \\ &= \sum_{m=0}^M [C_m(\theta) \cos(m\lambda) + D_m(\theta) \sin(m\lambda)] \end{aligned} \quad (7)$$

Time filtered anomalies of the other parameters ( $v$ ,  $z$ ,  $T$ ) are also produced in the same procedure. In cases of  $Z$  and  $T$ , 344 and 335 station data are adopted, respectively. To suppress artificially amplified anomalies over the data-sparse region, some (less than 10) bogus points with zero-anomalies are also added in each case. The

distribution of the original data (radiosonde station data, NMC grid-points data and bogus points) for  $U$  and  $V$  field is shown in Fig. 3.

#### 4. Assessment of analyzed data sets

There may be some doubt about the objectively analyzed data sets which are estimated with the limited degree of freedom as described in the previous section. In this section we present some results of assessment on the obtained time series and the spatial pattern.

In Fig. 4 original time-filtered data of temperature at 300 mb and zonal wind at 200 mb for some stations are compared to those of the adjacent grids deduced from the objective analysis. Although the analyzed data contain only the variances of limited zonal and meridional wavenumbers ( $m = 0$  to 5 with rhomboidal truncations), they could simulate, as a whole, the original data sufficiently. This fact may imply first that the anomalies of interannual time scales such as ENSO can be substantially composed with those of planetary-scale waves. However, the analyzed data also contain the statistical estimate errors due to insufficiency of data samples for the least-square method. For example, the analyzed data near Anchorage (Alaska) could simulate the original data substantially due to the sufficient data in the northern middle and high latitudes, but those at Alice Spring (Australia) have considerable estimate errors due to lack of station data in the southern hemisphere.

The stability of the analyzed data against the spatial truncations is also examined simply by comparing the spatial anomaly patterns deduced with different truncations. Fig. 5 shows the anomaly patterns of zonal wind at 200 mb for January 1973 deduced with the truncation of zonal wavenumber 0 to 5 (upper) and from that of zonal wavenumber 0 to 6 (lower). Though from place to place the anomaly wind speeds are more or less different each other (generally the values for  $m = 0-6$  are greater than those for  $m = 0-5$ ), the overall negative-positive pattern is quite similar with each other. It seems that only in some portions where the ENSO signals are less significant and also the original data are sparse such as over the southern oceans, considerable changes of anomaly pattern are apparent.

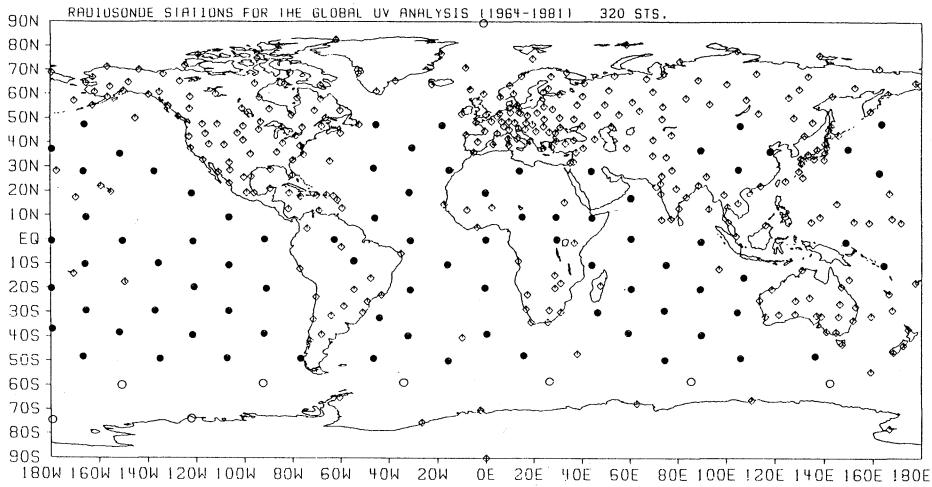


Fig. 3. Distribution of data points for the objective analysis of U and V. Cubic marks denote radiosonde stations, black dots denote the points adopted from NMC tropical operational wind analysis, and white dots denote zero-anomaly bogus points.

Thus, we may conclude that the objective analysis scheme we have employed here could fundamentally extract the ENSO related anomalies except some data sparse region such as the southern middle and high latitudes. This analysis scheme seems to function more efficiently for the time-filtered data sets.

### 5. Composite anomalies during El Niño

During the analysis period, one ENSO cycle shows nearly 4-year period particularly during 1964 to 1979. In fact, El Niño occurred in 1965, 1969, 1972/73 and 1976/77 and anti-El Niño conditions occurred in 1964, 1967/68, 1970/71, 1973/74, 1975/76 and 1978/79, as shown in Fig. 1. Although considerable decrease of SOI appeared during 1974/75, this phase did not show any characteristics of El Niño in the SLP nor wind field (Barnett, 1985; Gutzler and Harrison, 1986 etc.). Yasunari (1985) also suggested that this minor minimum of SOI may be associated with the tropospheric QBO. In the present analysis, therefore, we have chosen the time filter to smooth out this phase as possible.

We then categorized 8 phases for each ENSO cycle during 1964 through 1979, in reference to the smoothed SOI values. For example, category 1 (5) denotes the maximum (minimum) SOI phase, which corresponds with the El Niño (anti-El Niño) period. Similarly, category 3 (7) corre-

spond with the intermediate stage from the El Niño (anti-El Niño) to the anti-El Niño (El Niño) period. One category of each ENSO cycle has a 5 to 6 months time length.

To scrutinize the circulation, temperature and height anomalies over the whole global domain associated with the ENSO cycle, composite anomaly fields for each category are produced, by averaging the four (or five) cases during the analysis period (1964–79).

In this section, the global anomaly field of 10 parameters during El Niño period (category 5) are demonstrated.

#### a. SST

Composite SST anomalies during El Niño period (category 5) are shown in Fig. 6. Large positive anomalies exceeding  $0.6^{\circ}\text{C}$  are remarkably seen over the central through the eastern equatorial Pacific. Large area of negative anomalies are also apparent over the northern Pacific, which has been already pointed out as another significant feature of SST anomalies during El Niño (Weare *et al.*, 1976).

It is also noteworthy to state that positive anomalies are commonly seen over the whole tropical oceans except the western Pacific although the maximum amplitudes appear in the eastern Pacific. This has also been noted by Pan and Oort (1983) and Hsiung and Newell (1983).

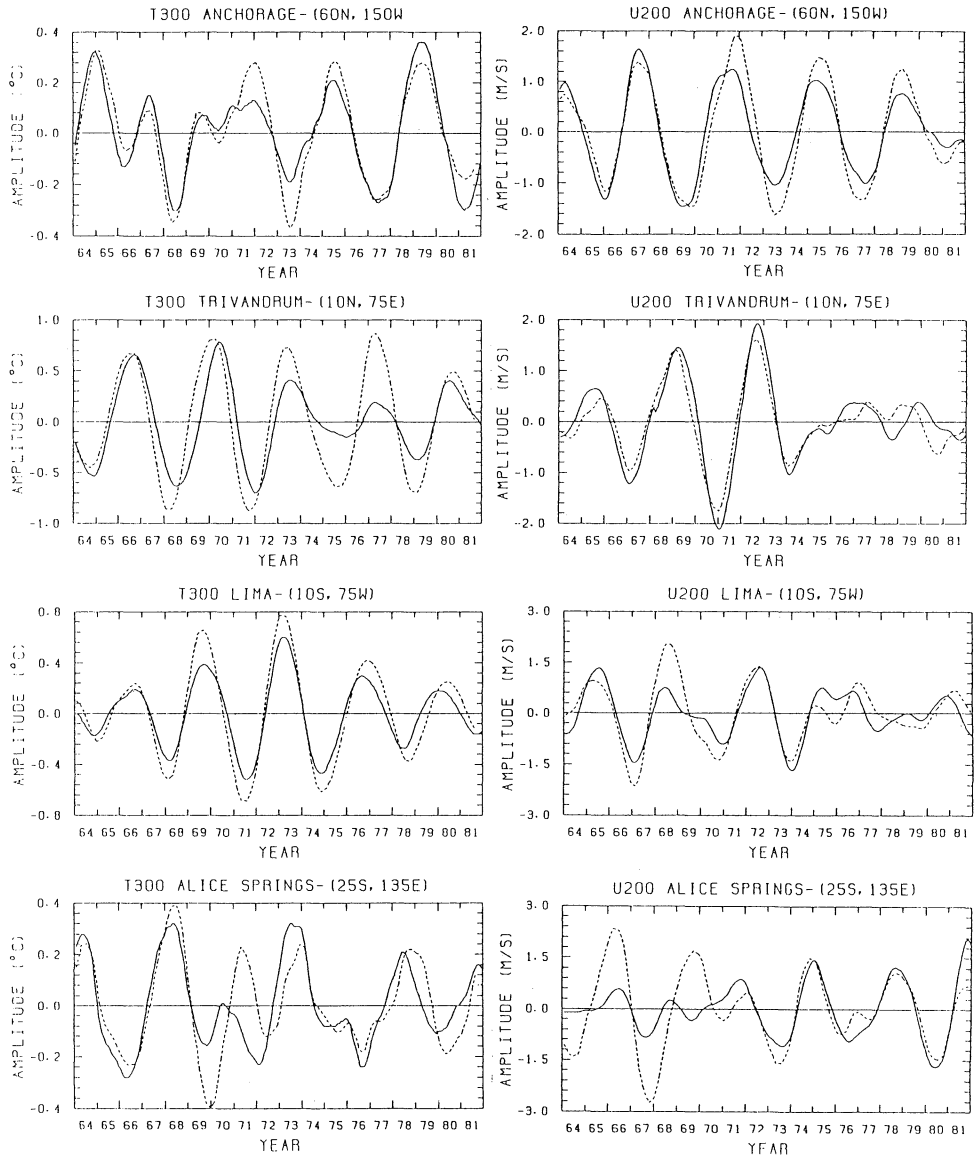


Fig. 4. Time-filtered data of temperature at 300 mb (left) and zonal wind at 200 mb (right) at four stations (dashed line) and objectively analyzed time filtered data at grids adjacent to these stations (solid line).

Negative anomalies over the southern Pacific to the south of about  $25^{\circ}\text{C}$  also seem to be significant, which may suggest a symmetric pattern of SST anomalies and associated atmospheric responses in the both sides of the equator.

#### b. SLP

Fig. 7 shows the composite SLP anomalies during El Niño. Since the SLP anomalies used

here are not normalized, large-amplitude anomalies tend to appear in higher latitudes. Yet, the east-west contrast of the anomalies in the low latitudes between Australia-Indonesian region and the eastern Pacific is a predominant pattern, which is evidenced as the SO. Large positive anomalies over Australia may imply the intensified subtropical high there, while the negative

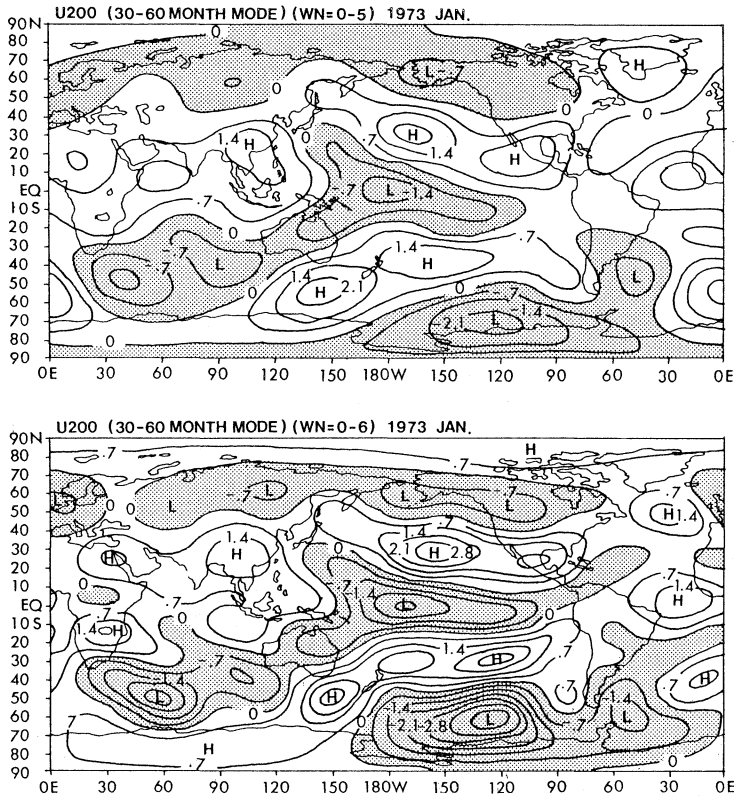


Fig. 5. Filtered anomaly zonal wind at 200 mb for January 1973 deduced with rhomboidal truncation of zonal wavenumber 0 to 5 (upper) and 0 to 6 (lower). Negative values are shaded. Units are  $0.7 m s^{-1}$ .

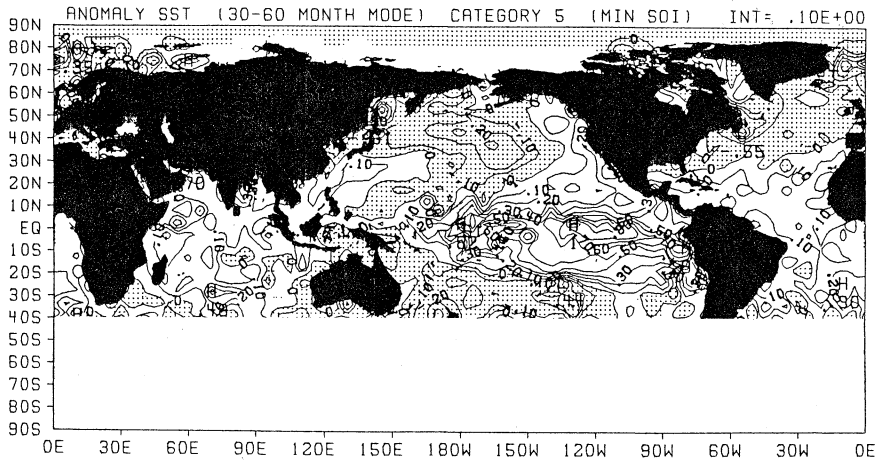


Fig. 6. Composite filtered anomaly distribution of sea surface temperature at category 5 (El Niño or minimum SOI phase). Units are  $0.1^{\circ}C$  and negative values are shaded. Data south of  $40^{\circ}S$  are not shown.

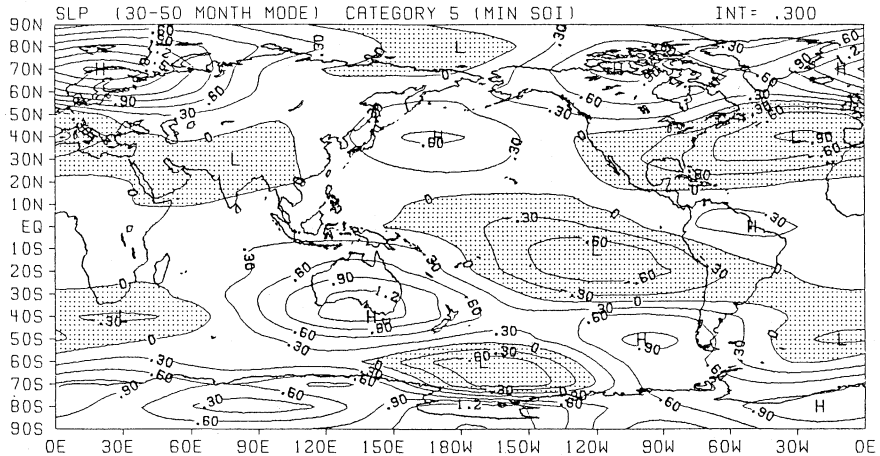


Fig. 7. Same as Fig. 6 but for sea level pressure. Units are 0.3 mb and negative values are shaded.

anomalies over the eastern Pacific and the elongated positive anomalies from Australia toward the southern tip of South America may suggest the weakened South Pacific high and associated north-eastward displacement of South Pacific Convergence Zone (SPCZ) during El Niño.

Another remarkable feature may be the north-south contrast of anomalies over Europe through the north Atlantic. This may be related to the North Atlantic Oscillation (NAO) signals (Walker and Bliss, 1932) though some studies (Barnett, 1985 etc.) noted that NAO and SO are not correlated each other in time series.

### c. Wind fields

Fig. 8 shows the composite anomalies of (a) zonal wind and (b) meridional wind at 200 mb during El Niño. In the zonal wind anomalies (Fig. 8(a)), the strong easterlies along the equatorial central Pacific and the strong westerlies to the north ( $30^{\circ}\text{N}$ – $50^{\circ}\text{N}$ ) and to the south ( $30^{\circ}\text{S}$ – $50^{\circ}\text{S}$ ) are noticeable. The westerlies are also broadly distributed in the low and middle latitudes over the Atlantic through Afro-Eurasia. Wind speeds of these anomalies exceeds  $2.0\text{ ms}^{-1}$  not only over the Pacific but also over the Indian Ocean. In the meridional wind anomalies (Fig. 8(b)), a symmetric wave-like pattern of northerly and southerly anomalies are prominently shown to the north and the south of the equatorial Pacific. In other areas of the world, however, no

systematic patterns can be found. The overall feature particularly of the zonal wind anomalies are nearly identical to the results by Arkin (1982) and Pan and Oort (1983).

Fig. 9 shows zonal wind anomalies at 700 mb. A prominent feature in the tropics is a coupling of the westlies over the central Pacific and the easterlies over the western Pacific through the Indian Ocean. This pattern is just opposite in the direction of wind to that at 200 mb over there (see Fig. 8(a)). That is, anomalous east-west circulation may be realized along the equatorial belt of this region as noted by Yasunari (1985). In the middle latitudes, in contrast, the westerlies seem to be distributed associated with those at 200 mb. In other words, baroclinic type zonal wind anomalies are dominant along the tropical belt most apparently over the Pacific, but equivalent barotropic-type wind anomalies are a characteristic feature in middle and high latitudes.

Anomalous heat source during El Niño may be located near to the westerly (easterly) maximum of 700 (200) mb over the central Pacific ( $180^{\circ}$ – $150^{\circ}\text{W}$ ) if we refer to simple linear theories (Matsuno, 1966; Gill, 1980).

To visualize the anomalous wind field more easily, streamline charts are produced as shown in Fig. 10. At 200 mb (Fig. 10(a)), an area of divergence over the central Pacific and two areas of convergence over the western Pacific and the Amazon basin are apparent. This pattern along



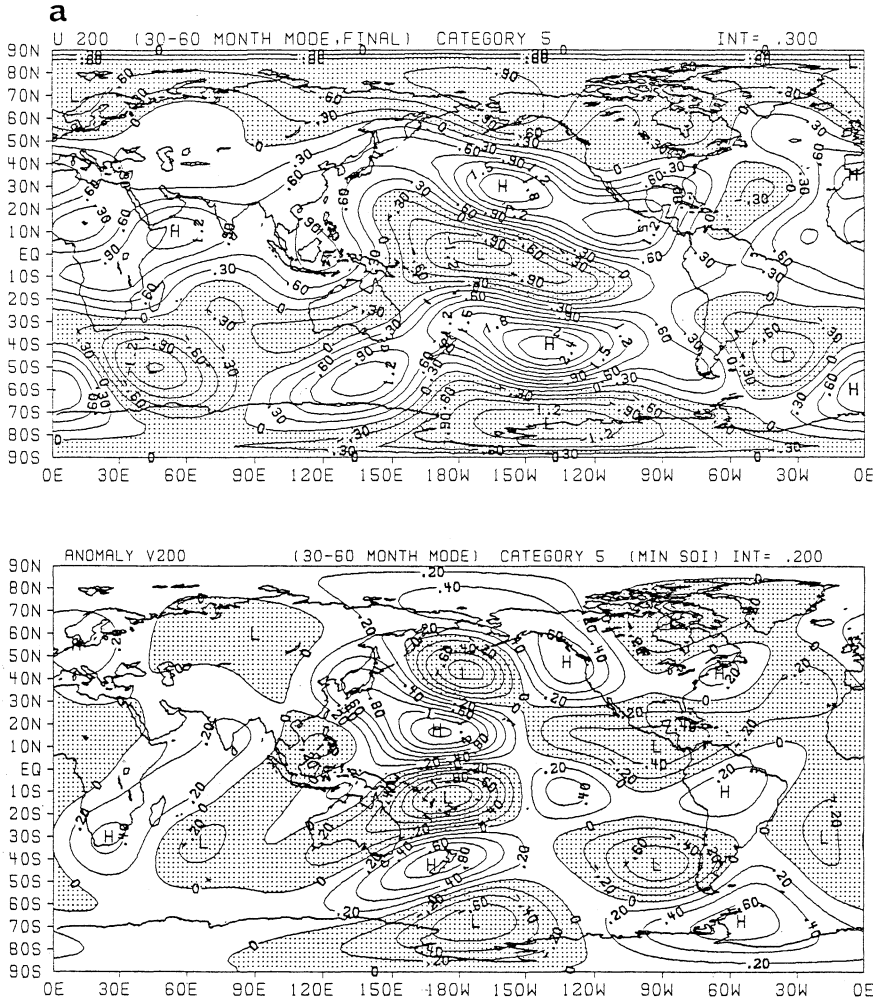


Fig. 8. Same as Fig. 6 but for (a) zonal wind at 200 mb and (b) meridional wind at 200 mb. Units are  $0.3 \text{ m s}^{-1}$  and  $0.2 \text{ m s}^{-1}$ , respectively. Negative values are shaded.

the equator is consistent well with the spatial pattern of anomalous convection (*i.e.*, strong convection over the former area and weak convections over the latter two areas) during 1982/83 El Niño (Ardanuy and Kyle, 1986).

A double anticyclonic-cell structure over the equatorial central Pacific and a cyclonic-cell structure to the north of it (*i.e.*, over the Aleutian low area) are evident. Another cyclonic circulation can also be identified over the southern Pacific, and these two cyclonic cells seem to have a symmetric structure with respect to the equator. This feature suggests a strong stationary wave response of the atmosphere in the low and

middle latitudes of the two hemispheres to the anomalous heating over the equatorial Pacific.

We also notice a weak anticyclonic curvature over Canada and cyclonic circulation to the southeast of it, which is identified as a so-called PNA pattern (Horel and Wallace, 1981). Another remarkable feature is a broad band of westerlies over the low and middle latitudes of the Atlantic and Afro-Eurasian region (refer to Fig. 8(a)), which may imply the intensified subtropical jet stream associated with El Niño events.

At 700 mb (Fig. 10(b)), westerlies are prominent over the tropical Pacific as already noted in Fig. 9. On either side of this westerly zone (*i.e.*,

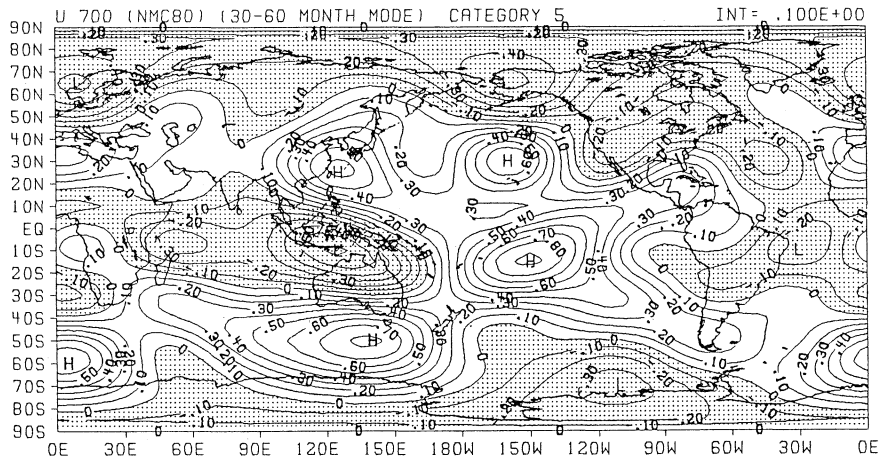


Fig. 9. Same as Fig. 6 but for zonal wind at 700 mb. Units are  $0.1 \text{ m s}^{-1}$  and negative values are shaded.

over the northern and the southern Pacific), two cyclonic circulations made a pair, which may suggest the response of the middle latitude westerlies to the anomalous heat source over the central Pacific. Over Australia, in contrast, a strong anticyclonic cell exist, which correspond to the intensified subtropical high over there and associated intensified easterlies over the Indonesian maritime continent.

#### e. Temperature and geopotential height in the upper troposphere

The anomalous thermal field in the atmosphere seems to be affected by the anomalous heating during El Niño most remarkably in the upper troposphere (e.g., Pan and Oort, 1983). Fig. 11 shows composite anomalies of (a) temperature at 300 mb and (b) geopotential height at 200 mb. A striking common feature in the two charts is a zonally-oriented positive anomalies in the low latitudes (roughly  $30^{\circ}\text{N}$ – $30^{\circ}\text{S}$ ) with a huge maximum over the central Pacific. In the middle latitudes of the two hemispheres, in contrast, negative anomalies are generally dominant. Areas of minimum anomalies are located over east Asia, northeast Pacific and western Europe in the northern hemisphere. The negative anomalies of temperature at 300 mb and 200 mb geopotential height over far east Asia may correspond to relatively cool summers during El Niño years (Kurihara, 1985). In the southern hemi-

sphere, patterns of negative and positive anomalies are rather erroneous, probably because of insufficient data particularly in the middle and higher latitudes. The overall feature in Fig. 11 suggests that the local Hadley-type circulation over the Pacific is so intensified during El Niño phase that the warming of the troposphere prevails over the whole tropical belt and the subtropical jet streams are intensified over the whole subtropics (Fig. 8(a)).

## 6. Summary and discussion

The anomalies of SST, SLP, wind, temperature and geopotential height fields during El Niño periods have been investigated over the whole globe, by using objectively analyzed time-filtered data sets. It was recognized anew that the ENSO should be viewed as a global-scale climate system rather than a local atmosphere-ocean coupled system over the equatorial Pacific Ocean although the anomalies over the Pacific are remarkably large.

It is noted that the positive SST anomalies over the equatorial Indian and Atlantic Ocean appear nearly in phase with the warm episode over the eastern Pacific. Warming of the upper troposphere in the whole tropics and the increasing of zonal winds in the subtropics and the middle latitudes of the two hemispheres are also prominent at the same time. These evidences apparently suggest that the Hadley-type circula-

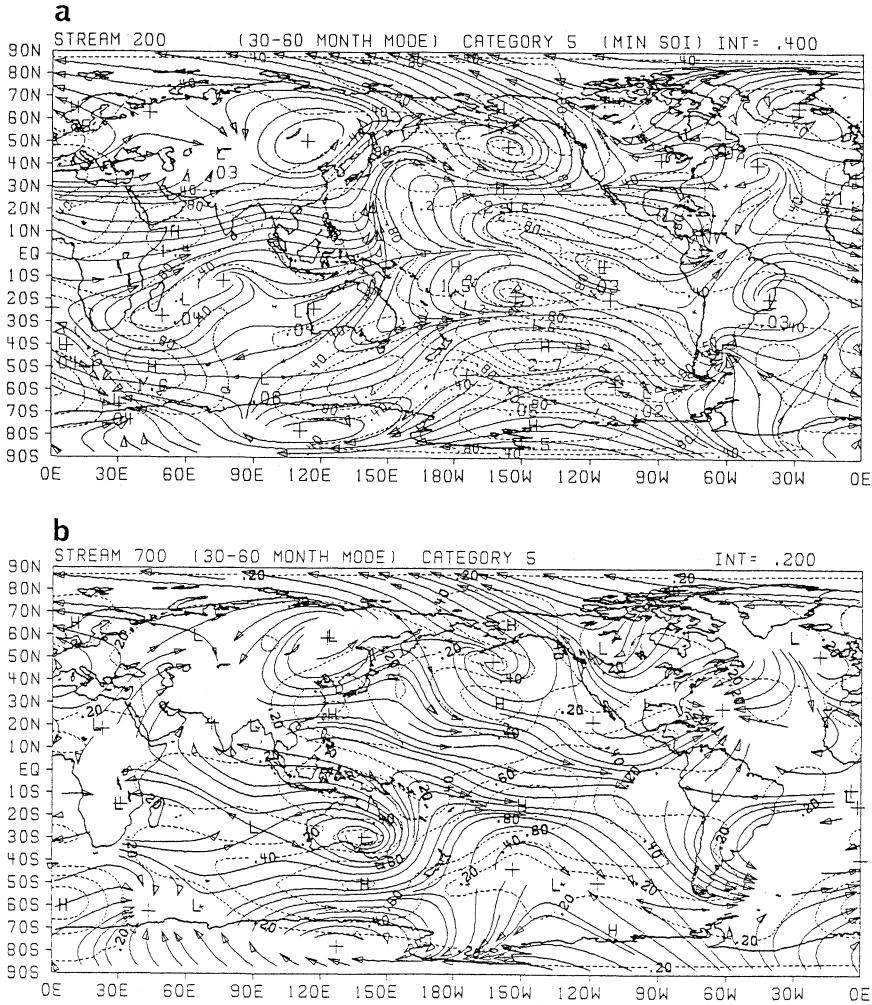


Fig. 10. Same as Fig. 4 but for (a) streamline at 200 mb and (b) streamlines at 700 mb. Contours of wind speed are shown with dotted lines. Units of wind speed are  $0.4 \text{ m s}^{-1}$  and  $0.2 \text{ m s}^{-1}$ , respectively.

tion is intensified during El Niño episodes most significantly over the central Pacific but also over the entire tropics. The results here are compatible with those by Pan and Oort (1983).

Another interesting feature is a nearly-symmetric response of the upper troposphere over the northern and the southern Pacific with the equatorial anomalous heating. Although most of the previous observational and theoretical studies stressed the response in the northern mid-latitudes (e.g., Horel and Wallace, 1981), the symmetric response pattern with respect to the equator has also been suggested (e.g., Branstator,

1985).

The NAO-type SLP anomalies over the north Atlantic seem to be consistent with the north-south contrast of anomalies of geopotential height (and temperature) in the upper troposphere. The negative SLP anomalies in the southern part and the positive SLP anomalies in the northern part imply the general weakening of Azores high and the southward shift of Icelandic low, which seems to be consistent with the negative anomalies of geopotential height, temperature and the positive anomalies of zonal wind in the upper troposphere of the southern part.

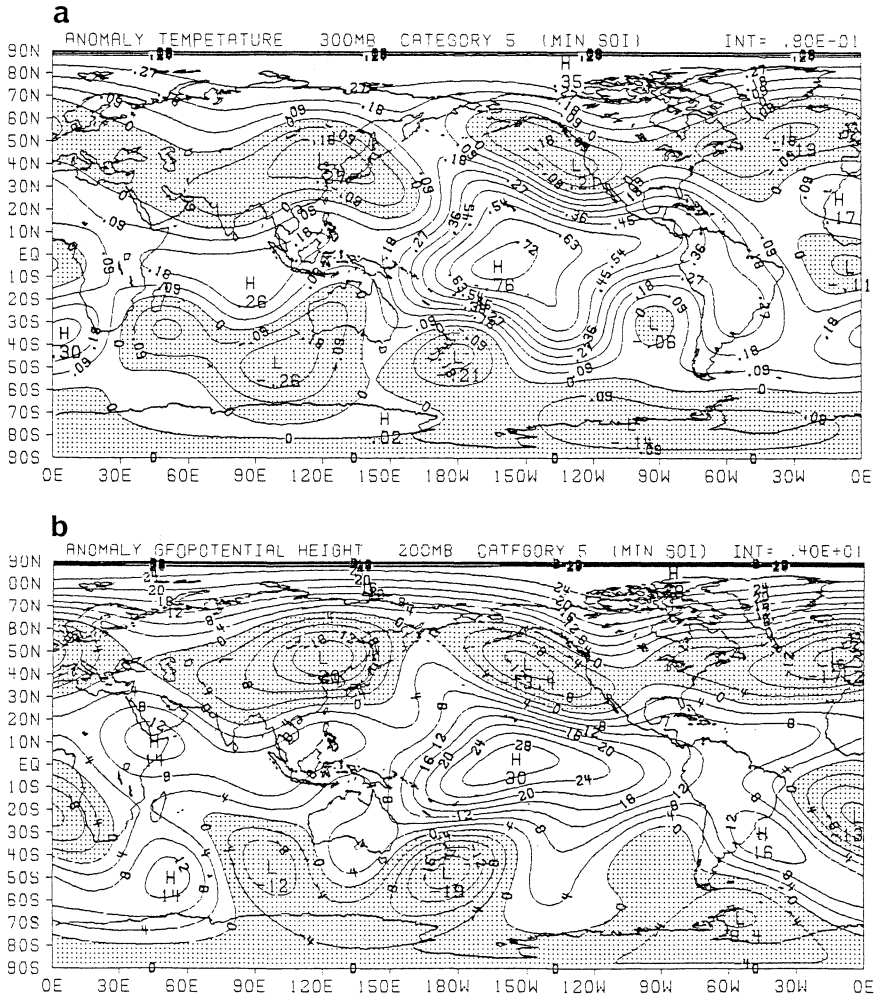


Fig. 11. Same as Fig. 4 but for (a) temperature at 300 mb and (b) geopotential height at 200 mb. Units are  $0.9^{\circ}\text{C}$  and 4 gpm, respectively. Negative values are shaded.

Barnett (1985) stressed the orthogonality of SO mode and NAO mode based on the CEOF analysis of SLP. However, the present results have suggested a strong association of NAO with SO as far as our analysis period (1964–79) is concerned. In fact, the two modes of Barnett (1985) seem to be well correlated each other during this period though they appeared to be independent each other through the whole period (1951–80) of his analysis.

In the present study, it has been revealed that objectively-analyzed time filtered data sets are effective to examine the global feature of ENSO related anomalies. The application of the time-

filtered series to truncated spherical harmonics (with  $m=0$  to 5) seems to have been efficient to extract this mode since ENSO may be a phenomenon of planetary-scale.

In the present paper, however, we have not discussed how the anomalies over the whole globe change in time associated with the evolution of ENSO cycles. This problem will be discussed in Part II of the present study.

#### Acknowledgements

The author would particularly thank Prof. T.N. Krishnamurti for his great support, encour-

agement and stimulating discussions throughout the work. He is also indebted to Dr. Eugene M. Rasmusson and Dr. P.A. Arkin for providing the NMC tropical wind data set. Thanks are due to Dr. T. Yamanouchi of National Institute of Polar Research for supplying some Antarctic station data. The research reported here is supported by NOAA Grant No. NA85AA-H CA019.

### References

- Anderson, D.L.T. and J.P. McCreary, 1985: Slowly propagating disturbances in a coupled ocean-atmosphere model. *J. Atmos. Sci.*, **42**, 615–629.
- Ardanuy, P.E. and H.L. Kyle, 1986: El Niño and outgoing longwave radiation: Observation from Nimbus-7 ERB. *Mon. Wea. Rev.*, **114**, 415–433.
- Arkin, P.A., 1982: The relationship between interannual variability in the 200 mb tropical wind field and the Southern Oscillation. *Mon. Wea. Rev.*, **110**, 1393–1404.
- Barnett, T.P., 1983: Interaction of the monsoon and Pacific trade wind system at interannual time scales. Part I: The equatorial zone. *Mon. Wea. Rev.*, **111**, 756–773.
- , 1984a: Interaction of the monsoon and Pacific trade wind system at interannual time scales. Part II: The tropical band. *Mon. Wea. Rev.*, **112**, 2380–2387.
- , 1984b: Interaction of the monsoon and Pacific trade wind system at interannual time scales. Part III: A partial anatomy of the Southern Oscillation. *Mon. Wea. Rev.*, **112**, 2388–2400.
- , 1985: Variations in near-global sea level pressure. *J. Atmos. Sci.*, **42**, 478–501.
- Bhalme, H.N. and S.K. Jadhav, 1984: The southern oscillation and its relation to the monsoon rainfall. *J. Climat.*, **4**, 509–520.
- Bjerknes, J., 1966: A possible response of the atmospheric Hadley circulation to equatorial anomalies of ocean temperature. *Tellus*, **18**, 820–829.
- , 1969: Atmospheric teleconnections from the equatorial Pacific. *Mon. Wea. Rev.*, **97**, 163–172.
- Blackmon, M.L., J.E. Geilser and E.J. Pitcher, 1983: A general circulation study of January climate anomaly patterns associated with interannual variation of equatorial Pacific sea surface temperatures. *J. Atmos. Sci.*, **40**, 1410–1425.
- Branstator G., 1985: Analysis of general circulation model sea-surface temperature anomaly simulations using a linear model. Part I: Forced solutions. *J. Atmos. Sci.*, **42**, 2225–2241.
- Gill, A.E., 1980: Some simple solutions for heat-induced tropical circulation. *Quart. J. Roy. Met. Soc.*, **106**, 447–462.
- and E.M. Rasmusson, 1983: The 1982–83 climate anomaly in the equatorial Pacific. *Nature*, **306**, 229–234.
- Gutzler, D.S. and D.E. Harrison, 1986: The structure and evolution of seasonal wind anomalies over the near-equatorial eastern Indian and western Pacific Oceans. submitted to *Mon. Wea. Rev.*
- Horel, J.D. and J.M. Wallace, 1981: Planetary-scale atmospheric phenomena associated with the Southern Oscillation. *Mon. Wea. Rev.*, **109**, 813–829.
- Hoskins, B.J. and D. Karoly, 1981: The steady linear response of a spherical atmosphere to thermal and orographic forcing. *J. Atmos. Sci.*, **38**, 1179–1196.
- Hsiung, J. and R.E. Newell, 1983: The principal non-seasonal modes of variation of global sea surface temperature. *J. Phy. Oceanogr.*, **13**, 1957–1967.
- Kurihara, K., 1985: Relationship between the surface air temperature in Japan and sea water temperature in the western tropical Pacific during summer. *Tenki*, **32**, 407–417 (in Japanese).
- Krishnamurti, T.N., S.H. Chu and W. Iglesias, 1986: On the sea level pressure of the Southern Oscillation. *Arch. Met. Geoph. Biocl.*, Ser. A, **34**, 385–425.
- Matsuno, T., 1966: Quasi-geostrophic motions in the equatorial area. *J. Met. Soc. Japan*, **44**, 25–43.
- Murakami, M., 1981: Large-scale aspects of deep convective activity over the gate area. *Mon. Wea. Rev.*, **107**, 994–1013.
- Namias, J., 1976: Some statistical and synoptic characteristics associated with El Niño. *J. Phys. Oceanogr.*, **6**, 130–138.
- Pan, H-L., 1979: Upper tropospheric tropical circulations during a recent decade. *Florida State University Report No. 79-1*. Department of Meteorology, FSU. 141 pp.
- Pan, Y-H. and A.H. Oort, 1983: Global climate variations connected with sea surface temperature anomalies in the eastern equatorial Pacific Ocean for the 1958–73 period. *Mon. Wea. Rev.*, **111**, 1244–1258.
- Pant G.B. and B. Parthasarathy, 1981: Some aspects of an association between the Southern Oscillation and Indian summer monsoon. *Arch. Met. Geoph. Biocl.*, Ser. B, **29**, 245–252.
- Philander, S.G.H., T. Yamagata and R.C. Pacanowski, 1984: Unstable air-sea interactions in the tropics. *J. Atmos. Sci.*, **41**, 604–613.
- Rasmusson, E.M. and T.H. Carpenter, 1983: The relationship between eastern equatorial Pacific sea surface temperatures and rainfall over India and Sri Lanka. *Mon. Wea. Rev.*, **111**, 517–528.
- Reynolds, R.W., 1983: A comparison of sea surface temperature climatologies. *J. Climat. App. Met.*, **22**, 447–459.
- Shukla, J. and J.M. Wallace, 1983: Numerical simulation of the atmospheric response to equatorial Pacific sea surface temperature anomalies. *J. Atmos. Sci.*, **40**, 1613–1630.
- van Loon, H. and D.J. Shea, 1985: The Southern Oscillation. Part IV: The precursors south of 15°S to the extremes of the oscillation. *Mon. Wea. Rev.*, **113**, 2063–2074.
- Walker, G.T. and E.W. Bliss, 1932: World weather V.

*Mem. Roy. Met. Soc.*, 4, 53–84.  
 Weare, B., A.R. Navato and R.E. Newell, 1976: Empirical orthogonal analysis of Pacific sea surface temperatures. *J. Phys. Oceanogr.*, 6, 671–678.  
 Yasunari, T., 1985: Zonally propagating modes of the

global east-west circulation associated with the Southern Oscillation. *J. Met. Soc. Japan*, 63, 1013–1029.  
 Zebiak, S.E. and M.A. Cane, 1985: A model ENSO. submitted to *J. Atmos. Sci.*

---

## ENSO (エル・ニーニョ/南方振動) の全球構造 第1部：エル・ニーニョ時の合成

安成 哲三\*

(フロリダ州立大学気象学教室)

18年間 (1964~1981) の客観解析された資料をもとに、ENSOに伴う海面水温と大気構造の全球的な変化を調べた。客観解析は320地点以上の高層観測資料と、NMC熱帯域風資料をもとに、最小自乗法で球面調和函数 (東西波数5で切断) を求める手法を用いた。

第1部では、エル・ニーニョ完熟期における海面水温と大気各要素の偏差パターンを記述した。この時期、海面水温と対流圏上層の気温は、赤道中・東部太平洋付近のみならず、全熱帯域で高くなること、これに対し中・高緯度では全般に低くなること、中緯度偏西風は両半球とも強化され、しかも低緯度側に偏位することが明らかとなった。これらの事実は、低緯度側でのハドレー循環の強化、高緯度側での極渦の拡大を示唆している。

南北両太平洋域における、熱源に対する大気の定常応答のパターンが、赤道に対称的であること、北大西洋振動 (NAO) と南方振動 (SO) との同期的変動の様相も示された。

---

\* 現在所属：筑波大学地球科学系